Liouville-Neumann series approach to the Lieb-Liniger model

Alexander Kormentzas

March 4, 2022

Contents

1 Introduction

Integrability is a mathematical property of certain dynamical systems. Generally speaking, an integrable systems consists of a dynamical system with sufficient many conserved quantities, i.e., the integrals of motion. Thus, the system's degrees of freedom are substantially lower than the dimensionality of its phase space, and its evolution is restricted. To characterize integrable systems, we often talk about three features; complete integrability, i.e. the existence of a maximal set of conserved quantities; algebraic integrability, i.e. the existence of algebraic invariants, having a base in algebraic geometry; and lastly, solvability, i.e. the determination of solutions for such a model in an explicit functional form. These systems do not necessarily have solutions that can be expressed in closed forms, and nowadays integrability functions as a property of the geometry or topology of the system's solutions in phase space.

Integrability as a concept dates back to Hans Bethe, whose work concerned the energy eigenstates of the 1-D Heisenberg spin chain with the nearest interaction, in 1931 [1]. Bethe proposed a special form of the wavefunction. This form consists of a superposition of all possible permutations of plane waves in a line of length L, namely $\chi = \sum_{\mathcal{P}} A(\mathcal{P}) e^{i(k_{\mathcal{P}_1} x_1 + \ldots + k_{\mathcal{P}_N} x_N)}$, where $\mathcal{P}_1 \ldots \mathcal{P}_N$ stand for a permutation $\mathcal{P}$ of integers $1, 2, \ldots N$ and $A(\mathcal{P})$ are the phase shifts. $N!$ plane waves are N-fold exponential phase factors $e^{ik_j x_j}$. This special form will be discussed more in section 2.

This solution, called Bethe's ansatz (BA), did not receive much popularity upon inception. However, in 1963, Lieb and Liniger [2, 3] first solved the 1-D many-body problem of bosons with a two-body delta-function interaction, using Bethe's hypothesis. They gave exact solutions for this model in terms of the wave numbers (also called quasi-momenta or rapidities), $k_i (i = 1, \ldots, N)$, satisfying a set of Bethe ansatz equations, called the Lieb-Liniger equations. To find the spectrum of the model, one needs to sum up all k_i^2.

The Bethe ansatz equations describe the roles of individual particles in many-body correlations. Thus, quantum integrability enters the playing field. To explain quantum integrability, one needs to consider a free particle setting, where all one-body dynamics are reducible. To name a quantum system integrable, the two-body dynamics must be reducible. One example is that of spin chains, while other interesting cases consist of interacting quantum gases, the Hubbard Model, Gaudin magnets, etc.

As previously mentioned, the reducibility of two-body interactions is a necessary condition to name a quantum model integrable. And that is exactly what C.N Yang [4] found in 1968 when working on the eigenvalue problem of the spin 1/2 δ-function interacting Fermi gas. To be precise, both C.N. Yang and Baxter [5] in 1971 independently found an equation that, if satisfied by a two-body scattering matrix of a system, made the system integrable. And of course, the equation took its name after both of them, namely, the Yang-Baxter equation. For models that satisfy this equation, meaning that they are exactly solvable, one can obtain the energy spectrum of the Hamiltonian exactly in terms of the BA equations. From there, one can proceed to derive physical properties of such a model. The Lieb-Liniger Bose gas [2] is a noteworthy BA integrable model, while another one is the Yang-Gaudin model [4, 6].

In 1969, C.N. Yang and C.P. Yang worked on the thermodynamics of the many-body problem [7]. They presented a grand canonical description of the model, in equilibrium. By minimizing the Gibbs free energy, the so called Yang-Yang equations arise, through which analytical solutions can be obtained. This Yang-Yang approach advanced our understanding of many-body physics, and has aided researches in finding exact solutions for finite temperatures, as well as other temperature regimes.

At this point, it is wise to discuss ensemble statistics, as we wish to properly distinguish the physical origin of distinguishable and indistinguishable particles. At room temperature, one can treat the particles in the air as N identical billiard balls (the well-known 1-D classical billiard or hard rod gas), colliding with each other, their size being much smaller than the mean distance between them. The particles are distinguishable. However, de Broglie matter-wave theory states that the thermal wavelength of a moving particle is given by the formula: $\lambda_{dB} = \sqrt{2\pi\hbar^2/(mk_BT)}$, where m is the mass of the particle, $\hbar$ is the Plank constant, k_b is Boltzmann's constant and T is the temperature. In the case we are discussing, as the temperature becomes very low, the thermal de Broglie wavelength increases, and the wave packets start to overlap with each other. Therefore, we can define a degenerate temperature, below which the particles are indistinguishable from one another. Below the degenerate temperature, the properties of fermions and

bosons differ, fundamentally. Fermions are subject to the Pauli exclusion principle, i.e. they cannot occupy the same quantum state. Bosons, however, obey no such principle, as under certain conditions they can collapse into the same quantum ground state, the famous Bose-Einstein condensate. The Lieb-Liniger model is an ideal ensemble to understand this physical disparity between the distinguishable and indistinguishable natures of classical and quantum particles. This becomes prominent when one investigates the different temperature regimes of the Lieb-Liniger model, and understands how the 1-D confined bosons behave in them.

Lately, the Bethe ansatz approach has been very successful in the realm of condensed matter physics, such as in Kondo impurity problems, BCS pairing models, the 1-D Hubbard model, spin ladders, quantum optics, cold atoms, quantum statistical mechanics and more. Recent research has shown remarkable connections between conformal field theory and Yang-Baxter integrability in 2D lattice models. In our work, we will explore the exactly solvable Lieb-Liniger model, utilizing the Bethe ansatz as well as the Yang-Yang equations.

We organize our work as follows. In Section 2, we present a derivation of the Bethe ansatz for the Lieb-Liniger Bose gas. We explore the limits of the model, from weak to strong coupling, providing insight on the various cases of excitations and interactions that commonly occur, discussing the model's spectrum. In Section 3, we provide a phase diagram for the model and give an in depth review of the Yang-Yang thermodynamics method, which we then use to extract results for the various limiting thermodynamical cases of the model, namely the different temperature and interaction strength regimes. In Section 4, we briefly discuss Generalized Hydrodynamics and its impact as a newly developed theory, providing an application of it on the Lieb-Liniger model.

2 The Lieb-Liniger model

The Lieb-Liniger model [2, 3] describes a system of N indistinguishable spinless bosons, interacting via a delta-function potential on a line of length L. The Hamiltonian of this system is:

$$\mathcal{H} = -\frac{\hbar^2}{2m}\sum_{i=1}^{N}\frac{\partial^2}{\partial x_i^2} + 2c\sum_{i<j}^{N}\delta\left(x_i - x_j\right) \tag{1}$$

where c is the interaction strength and x_i refers to the position of the particles. From here forward, we will work in the units $\hbar = 2m = 1$ for convenience.

Lieb and Liniger [3] used a BA of the wavefunction-superposition of all possible permutations that plane waves in a line of length L can have, namely:

$$\chi = \sum_{\mathcal{P}} A(\mathcal{P}) e^{i(k_{\mathcal{P}_1}x_1 + \ldots + k_{\mathcal{P}_N}x_N)}, \quad A(\mathcal{P}') = \frac{k_{\mathcal{P}_j} - k_{\mathcal{P}_{j+1}} + ic}{k_{\mathcal{P}_j} - k_{\mathcal{P}_{j+1}} - ic} A(\mathcal{P}) \tag{2}$$

where $\mathcal{P}_1 \ldots \mathcal{P}_N$ stand for a permutation $\mathcal{P}$ of integers $1, 2, \ldots N$. $N!$ plane waves are N-fold exponential phase factors $e^{ik_j x_j}$. The N wave numbers k_i permute among the N coordinates x_j. We call k_i rapidities or quasi-momenta. In addition, the whavefunction (2) is allowed a global phase $e^{i\alpha}$, with $\alpha = 0$ making the wavefunction periodic, while $\alpha = \pi$ makes it anti-periodic.

Applying periodic boundary conditions $\alpha = 0$ to (2) that obey the Hamiltonian (1), we arrive at the Bethe equations, a set of N equations for N particles:

$$e^{ik_j L} = \prod_{l\neq j}^{N} \frac{(k_j - k_l) + ic}{(k_j - k_l) - ic}, \quad j = 1, 2, \ldots, N \tag{3}$$

It is convenient to take the logarithm of these Bethe equations (3) to obtain:

$$k_j = \frac{2\pi}{L} I_j - \frac{1}{L} \sum_{l=1}^{N} \theta(k_j - k_l) \tag{4}$$

where the quantum numbers I_j are in one to one correspondence with the rapidities k_j [3, 7], and:

$$\theta(k) = i \ln \left(\frac{ic + k}{ic - k} \right) \tag{5}$$

To obtain the ground state, one sets:

$$I_j = j - \frac{N+1}{2}, \qquad j = 1, 2, \ldots, N \tag{6}$$

All other combinations with mutually distinct I_j, where I_j are integers (half-integers) in the case of N odd (even) lead to allowed solutions of the Bethe equations and constitute excited states. In the ground state the I_j's are all different (so are the rapidities k_j) and symmetrically distributed around 0, leading to the configuration resembling a Fermi sea.

2.1 Thermodynamic Limit at $T = 0$

If we order the quantum numbers I_j (and therefore the rapidities k_j) in increasing order, we can write the Bethe equations (4) as:

$$k_j - \frac{1}{L} \sum_{l=1}^{N} \theta(k_j - k_l) = g(k_j) \tag{7}$$

where we define the counting function $g(k)$ as an arbitrary function constrained only by two properties: 1) It must be monotonically increasing; 2) It must take the value of a quantum number at the corresponding quasi-momentum $g(k_j) = \frac{2\pi}{L} I_j$ when $\theta(k) \to 0$. Now, we can take the limit $N, L \to \infty$, keeping the density N/L fixed and finite. We introduce the density of rapidities:

$$\rho\left(k_j\right) = \frac{1}{L(k_{j+1} - k_j)} \tag{8}$$

In the thermodynamic limit for an arbitrary function $g(k_j)$:

$$\sum_{j=1}^{N} g(k_j) \to L \int_{-\Lambda}^{+\Lambda} dk \rho(k) g(k) \tag{9}$$

Here, the parameter Λ plays the role of a momentum cut-off limit, where all states with $|k| < \Lambda$ are occupied and all states with $|k| > \Lambda$ are empty. The value of Λ (and therefore, the limits of integration) is determined through the particle number density (for a constant number density, meaning that this regime lies within the zero temperature limit):

$$\int_{-\Lambda}^{+\Lambda} dk \rho(k) = \frac{N}{L} = n \tag{10}$$

To get the thermodynamic limit of the Bethe equations for the ground state, we substitute Eq. (6) into Eq. (4) and take the difference of the equations with the indices $j + 1$ and j:

$$k_{j+1} - k_j = \frac{2\pi}{L} - \frac{1}{L}\sum_{l=1}^{N}[\theta(k_{j+1} - k_l) - \theta(k_j - k_l)] \tag{11}$$

Since the difference $k_{j+1} - k_j$ is small in the thermodynamic limit, we can rewrite Eq. (11) as follows:

$$k_{j+1} - k_j = \frac{2\pi}{L} - \frac{k_{j+1} - k_j}{L}\sum_{l=1}^{N}\theta'(k_j - k_l), \quad N, L \to \infty \tag{12}$$

where $\theta'(k) = \frac{\partial\theta(k)}{\partial k}$. Now, using Eqs. (8) and (9), we obtain:

$$\rho(k) = \frac{1}{2\pi} + \frac{1}{2\pi}\int_{-\Lambda}^{+\Lambda} d\lambda\rho(\lambda)K(k,\lambda), \quad -\Lambda \leq k \leq \Lambda \tag{13}$$

where:

$$K(k,\lambda) = \theta'(k-\lambda) = \frac{2c}{c^2 + (k-\lambda)^2} \tag{14}$$

and Λ again is the momentum cut-off, which in the $c \to \infty$ limit of the 1D Lieb-Liniger Bose gas becomes a Fermi momentum with $\Lambda = k_F = \pi n$. The various cases for the interaction strength will be discussed in later sections. The linear integral equation (13) is called the Lieb-Liniger equation and can be solved together with the normalization condition (10) to give the rapidity distribution function $\rho(k)$. All the thermodynamic parameters can be calculated from $\rho(k)$ and Λ. The ground state energy and the particle number per unit length in the canonical ensemble are:

$$e = \int_{-\Lambda}^{+\Lambda} k^2\rho(k)dk, \quad n = \int_{-\Lambda}^{+\Lambda}\rho(k)dk \tag{15}$$

We can make the following changes to our parameters:

$$k = \Lambda x, \quad c = \Lambda\zeta, \quad \rho(\Lambda x) = g(x) \tag{16}$$

and rewrite Eqs. (13) and (15) respectively, as:

$$g(x) = \frac{1}{2\pi} + \frac{1}{2\pi}\int_{-1}^{+1} dz\frac{2\zeta g(z)}{\zeta^2 + (x-z)^2} \tag{17}$$

$$e = \frac{c^3}{\zeta^3}\int_{-1}^{+1} g(z)z^2dz \tag{18}$$

$$n = \frac{c}{\zeta}\int_{-1}^{+1} g(z)dz \tag{19}$$

2.2 Limits of the model and the γ parameter

In this section, we discuss the results Lieb and Liniger portrayed in regards to the limit of the model. The limits depend on the values the dimensionless parameter $\gamma = \frac{c}{n}$ obtains, as well as on the parameter's relation to the density function. Such study is accomplished through the use of equations (16) – (18), by solving Eq. (17) for fixed ζ, then using Eq. (19) to determine ζ as a function of γ, and finally obtaining e as a function

of γ through Eq. (18). In addition, one can obtain the potential and kinetic energy per particle through the solution of (16) − (18) via the formuli $U = n^2\gamma\frac{de}{d\gamma}, T = n^2\left(e - \gamma\frac{de}{d\gamma}\right)$.

We will not go into great detail about this method, but it is important to note the following: since Eq. (17) is an inhomogenous Fredholm equation of the second kind with an inhomogenous term that is positive definite, Lieb and Liniger have proven that $g(x)$ is unique for any inhomogenous term and analytic for $\zeta > 0$. Consequently, if the inhomogenous term is positive definite, $g(x) > 0$ for all x, and if it is also bounded above (below), then $g(y)$ is bounded above (below). Thus, Lieb and Liniger prove that $g(x, \gamma)$, $e(\gamma)$, ζ and also the cut-off Λ are analytic functions of γ, except in the case $\gamma = 0$, allowing smooth evaluation of thermodynamical quantities using numerical methods.

However, the severe singularity at $\gamma = 0$ has a physical meaning. Any volume-dependant interaction, however weak, leads in the limit of a large system to a system that is in some way basically different from the noninteracting case. One may attempt to procure a series of $e(\gamma)$ for small γ, but such a series can at best be asymptotic. In this regime of the singularity $\gamma = 0$, numerical calculations are extremely difficult, especially as one approaches the exact zero value of γ more and more.

Below, we present and discuss a graph found in the original work of Lieb and Liniger [2], plotting density distribution function $\rho(k)$ ($\rho(k) = f(k), n = \rho$ and $\Lambda = K$ in their work) for various values of quasi-momenta over numeric density $\frac{k}{n}$ in the ground state . They plot numerical results in units $n = 1$, so that $\frac{\Lambda}{n}$ obtains values between 0 and π, also eliminating the dependant parameter ζ through the aforementioned method. After discussing the results of their calculations, we shall close this section with a review of the large and small γ limits along with various quantities.

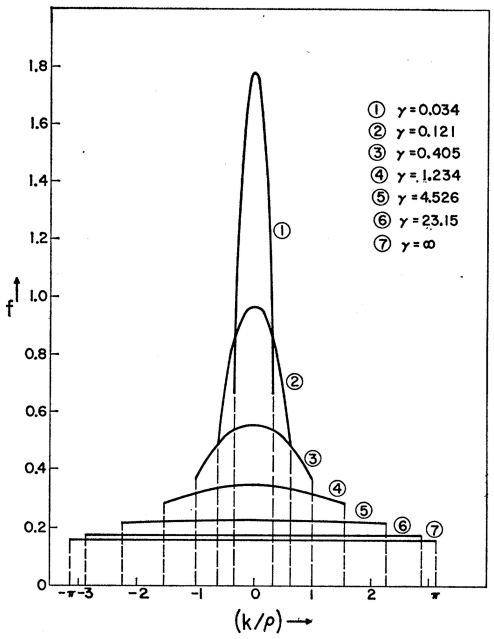

FIG. 2. The distribution function of "quasi-momenta" in the ground state for various values of $\gamma = c/\rho$. The vertical dashed lines are the cutoff momenta K (cf. Fig. 1). When $\gamma = \infty$, $f = (2\pi)^{-1}$. For all γ, $\int_{-K}^{K} f(k)dk = \rho$.

As is evident, for $\gamma \to 0$, the small values of the quasi-momenta k become more important. For these values we reach a limit called the semicircle law. In contrast, moving to large values $\gamma \to \infty$ shows that the density distribution function $\rho(k)$ approaches a static value $\frac{1}{2\pi}$. In this limit the gas is called Tonks-Girardeau (TG) gas. Both limits will be discussed more in later sections, as well as what the actual limiting values of γ are. For in-between, non-extreme values of γ, the density distribution function obeys Eq. (19).

For large γ, the denominator in the integral of Eq. (17) approaches the value ζ^2, and can be replaced by it, at the cost of a small error (compared to the numerical unit). This substitution demands $g(x) =$ const, which allows the evaluation $g(x) = \frac{\zeta}{2\pi\zeta - 4}$. Using this result to solve Eq. (18) and (19) leads to $\zeta = \frac{\gamma+2}{\pi}, e = \frac{\pi^2}{3}\left(\frac{\gamma}{\gamma+2}\right)^2, \Lambda = \frac{\pi n \gamma}{\gamma+2}$. The potential and kinetic energies per particle respectively are $U = \frac{4n^2 e}{\gamma+2}, T = \frac{\gamma-2}{\gamma+2} n^2 e$.

For small γ, Lieb and Liniger have shown that as $\zeta \to 0$, the inhomogenous term of Eq. (17) becomes an eigenvalue of the integral equation. Furthermore, $g(x, \zeta)$ has a singularity at $\zeta = 0$ and the integral kernel becomes unstable. Therefore, it is recognized that as $\zeta \to 0$, the kernel becomes $2\pi\delta(x - y)$ so that in this limit Eq. (17) transforms into $g(x) = g(x) + \frac{1}{2\pi}$, and $g(x)$ becomes unbounded. No simple ways to get a systematic reliable expression of $g(x)$ at $\zeta \to 0$ exist, but one can guess the zeroth order form: $g(x, \zeta) \sim \frac{(1-x^2)^{1/2}}{2\pi\zeta}$. Then, it can be shown that the corrections to this result are of higher order in ζ for all x, while also being positive definite. Another major difficulty, is deciding the nature of the end points $|x| = 1$. These results however, gives the small γ calculated quantities: $\zeta = \frac{1}{2}\sqrt{\gamma}, e = \gamma, \Lambda = 2n\sqrt{\gamma}$. The potential and kinetic energies per particle respectively are $U = \gamma, T = 0$.

An interesting and important observation is that for small γ the potential energy dominates the kinetic, while for large γ this is reversed. For $\gamma \to \infty$, one sees that $U \to 0$. This behavior extends to three dimensions and it is often said that a large potential behaves like a kinetic energy barrier. This fact supposedly stems from the ability of particles to "go around" each other in three dimensions, but we see that the phenomenon exists in one dimension as well, and the difference does not lie here.

2.3 Weak Coupling Limit: Semicircle Law

In this section, we discuss the weak coupling limit of the model, i.e., $Lc \ll 1$. For convenience, we will use the γ parameter one finds in literature to provide some insight.

In this case for the model, the Bethe Ansatz roots comprise a semi-circle law, with Gaudin [8] and several other groups [9, 10] noticing this kind of distribution. Using Hutson's method , Gaudin found the energy distribution function (17) and energy density (18):

$$g(x) \approx \frac{\Lambda}{2\pi c}\left(1 - x^2\right)^{1/2} + \frac{1}{4\pi^2}\left(1 - x^2\right)^{-1/2}\left(x \ln\frac{1-x}{1+x} + \ln\frac{16\pi e\Lambda}{c}\right)$$

$$e = n^3\left(\gamma - \frac{4}{3\pi}\gamma^{3/2}\right)$$

These results coincide with perturbative calculations made using the Bogoliubov method. In addition, a solution for the distribution function $\rho(k)$ has been obtained (through communications with Bortz M, privately [11]):

$$\rho(k) \approx \frac{1}{\pi}\frac{1}{\sqrt{\gamma}}\left(1 - \frac{k^2}{\Lambda^2}\right)^{1/2} + \mathcal{O}\left(\frac{1}{Lnc}\right)$$

where the cut-off $\Lambda = 2\sqrt{nc}$ is obtained by Eq. (10). We can see that the quasi-momentum distribution satisfies a semi-circle law where the cut-off is the radius of the circle, presented better below in Figure (1) .

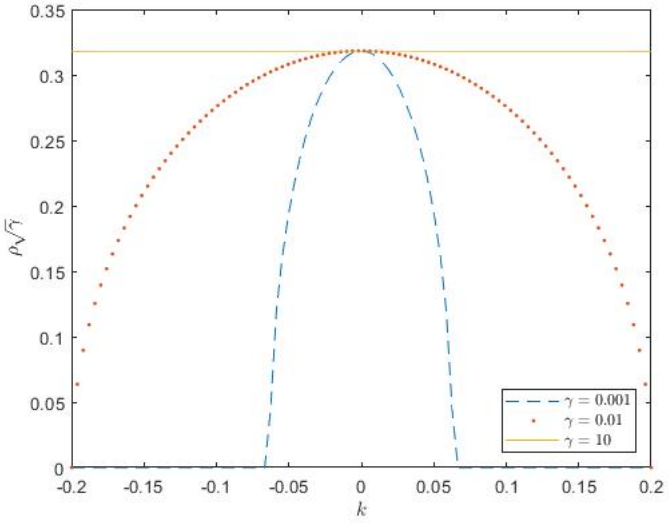

Figure 1: The quasi-momentum distribution ρ as a function of the quasi-momenta for various γ, n =1. We see that when γ is small, the distribution function meets a semi-circle law. For large γ, i.e., $\gamma \gg 1$, ρ becomes flatter and flatter, approaching a static value. We plot $\rho\sqrt{\gamma}$ for convenience.

2.4 Strong Coupling Limit (TG): Fermionization

In this subsection, we discuss the strong coupling limit, where the gas is known as the Tonks-Girardeau (TG) gas. In experiments with cold atoms, one can observe the degenerate gas with the strong coupling regime . In this regime of $\gamma \to \infty$, there exists a Bose-Fermi mapping method that maps the ground state properties of the Bose gas through the wavefunction of non-interacting fermions [12].

For finitely large γ, one can obtain the pseudo-momenta from the Bethe ansatz equations (3) [13]:

$$k_j = 2\pi \frac{I_j}{L}\left(1 - \frac{2}{\gamma} + \frac{4}{\gamma^2} - \frac{8}{\gamma^3}\right) + \frac{4\pi^3}{3c^3L^4}\left[\left(N + \frac{1}{2} - j\right)^4 - \left(\frac{1}{2} - j\right)^4\right] + O\left(\frac{1}{c^5}\right)$$

where I_j take the ground-state quantum numbers $I_j = -\frac{N-1}{2} + j - 1, j = 1, \ldots, N$. Using the above result, the ground-state energy of the strong repulsive gas is given by:

$$\frac{E}{L} \approx \frac{\pi^2}{3}n^3\left[1 - \frac{4}{\gamma} + \frac{12}{\gamma^2} + \frac{32}{\gamma^3}\left(\frac{\pi^2}{15} - 1\right)\right]$$

We could go in depth to explain the Fermi-Bose mapping, but it is enough to see that for $\gamma \to \infty$, the leading order of the ground state energy reduces to that of free fermions, i.e, $e_f = \frac{\pi^2 n^3}{3}$. For example, consider Eq. (6) describing the quantum numbers I_j. If we set $N = 13$ of the ground state in this limit, the I_j's obtain values $-6, -5, -4, -3, -2, -1, 0, 1, 2, 3, 4, 5, 6$, distinctively arranging themselves and corresponding to the rapidities k_j that obtain values $k_j = \frac{2\pi}{L}I_j$, coinciding with free fermions momenta. In the $\gamma \to \infty$ limit, one can picture these I_j's as bosons living in a 1D line, the delta function interaction between them forbidding them from passing each other and change places. Each boson's motion is strongly correlated to that of its two neighbours.

2.5 One-particle excitations

The ground state rapidity distribution in the N - particle sector of the Bose gas, which is not degenerate, is given by :

$$k_j = \frac{2\pi}{L}\left(j - \frac{N+1}{2}\right), \quad j = 1, ..., N \tag{20}$$

while in the $N+1$ - particle sector it is given by:

$$\tilde{k}_j = \frac{2\pi}{L}\left(j - \frac{N+2}{2}\right), \quad j = 1, ..., N+1 \tag{21}$$

As a result, we see that every $\tilde{k}_j$ is shifted by π/L with respect to k_j. We can avoid dealing with this shift by imposing anti-periodic boundary conditions in the $N+1$ - particle sector. Then the ground state rapidity distribution becomes:

$$\tilde{k}_j = \frac{2\pi}{L}\left(j - \frac{N+1}{2}\right), \quad j = 1, ..., N+1 \tag{22}$$

It is important to note that the ground state is 2 - fold degenerate, with another configuration corresponding to $j = 0, 1, ..., N$. While the choice of the anti-periodic boundary conditions eliminates the π/L shift, its influence onto the ground state energy is negligibly small (vanishes $\sim 1/N$) in the large N limit.

Now, the particle excitations can be decomposed into the "topological" part (boundary conditions change) and "truly one-particle" excitation. The Bethe equations are respectively:

$$\tilde{k}_j = \frac{2\pi}{L}\left(j - \frac{N+1}{2}\right), \quad j = 1, ..., N \tag{23}$$

and

$$\tilde{k}_{N+1} = \frac{2\pi}{L}M, \quad |M| > \frac{N}{2} \tag{24}$$

By comparing Eqs. (20) and (23), we see that $\tilde{k}_j = k_j$ for $j = 1, ..., N$.

2.6 One - particle shift

Consider the N - particle ground state given by Eq. (4). Then, add one particle and impose anti-periodic boundary conditions to obtain the Bethe equations:

$$\tilde{k}_j = \frac{2\pi}{L}\left(j - \frac{N+1}{2}\right) - \frac{1}{L}\sum_{l=1}^{N}\left[\theta\left(\tilde{k}_j - \tilde{k}_l\right) + \theta\left(\tilde{k}_j - \tilde{k}_{N+1}\right)\right], \quad j = 1, ..., N \tag{25}$$

$$\tilde{k}_{N+1} = \frac{2\pi}{L}M\sum_{l=1}^{N}\theta\left(\tilde{k}_{N+1} - \tilde{k}_l\right), \quad |M| > \frac{N}{2} \tag{26}$$

Taking the difference of Eqs. (4) and (25), we obtain:

$$L\left(k_j - \tilde{k}_j\right) + \sum_{l=1}^{N}\left[\theta\left(k_j - k_l\right) - \theta\left(\tilde{k}_j - \tilde{k}_l\right)\right] - \theta\left(\tilde{k}_j - \tilde{k}_{N+1}\right) = 0 \tag{27}$$

Using the fact that in the thermodynamic limit $k_{j+1} - k_j \sim 1/L$, we get:

$$\begin{aligned}\sum_{l=1}^{N} \left[\theta\left(k_j - k_l\right) - \theta\left(\tilde{k}_j - \tilde{k}_l\right)\right] \\ = \left(k_j - \tilde{k}_j\right) \sum_{l=1}^{N} \theta'\left(k_j - k_l\right) - \sum_{l=1}^{N} \left(k_l - \tilde{k}_l\right) \theta'\left(k_j - k_l\right), \quad N, L \to \infty\end{aligned} \tag{28}$$

Now, from Eq. (4) we see that:

$$\left(k_{j+1} - k_j\right) \left[L + \sum_{l=1}^{N} \theta'\left(k_j - k_l\right)\right] = 2\pi, \quad N, L \to \infty \tag{29}$$

We now define the shift function $J\left(k_j, k_{N+1}\right)$ as follows, denoting k_{N+1} as k_p to lighten the notation:

$$J\left(k_j, k_p\right) = \frac{k_j - \tilde{k}_j}{k_{j+1} - k_j} \tag{30}$$

Using Eqs. (28-30), we can obtain from Eq. (27) an integral equation for the shift function:

$$J\left(k, k_p\right) = \frac{1}{2\pi} \int_{-\Lambda}^{\Lambda} d\lambda K(k, \lambda) J\left(\lambda, k_p\right) - \frac{1}{2\pi} \theta\left(k_p - k\right) \tag{31}$$

2.7 Momentum and Energy of the excited state

We introduce the dressed momentum $p(k)$ [14] by the formula:

$$p(k) = k + \int_{-\Lambda}^{\Lambda} d\lambda \rho(\lambda) \theta(k - \lambda) \tag{32}$$

Now, we wish to calculate the momentum difference $\Delta P\left(k_p\right)$ between the N - particle ground state and the $N + 1$ - particle excited state. It is obtained by:

$$\Delta P\left(p_p\right) = \sum_{l=1}^{N} \left(\tilde{k}_l - k_l\right) + k_p = -\sum_{j=1}^{N} J\left(k_j, k_p\right)\left(k_{j+1} - k_j\right) + k_p \to -\int_{-\Lambda}^{\Lambda} dk J\left(k, k_p\right) + k_p, \quad N \to \infty \tag{33}$$

Now, by multiplying both parts of Eq. (31) by $\rho(k)$, integrating over k and using the Lieb-Lienger equation (13), we get the identity:

$$\int_{-\Lambda}^{\Lambda} dk J\left(k, k_p\right) = -\int_{-\Lambda}^{\Lambda} dk \rho(k) \theta\left(k_p - k\right) \tag{34}$$

which ultimately results in:

$$\Delta P\left(k_p\right) = p\left(k_p\right), \quad \left|k_p\right| \geq \Lambda \tag{35}$$

Next, we introduce the dressed energy $\varepsilon(k)$ [14]:

$$\varepsilon(k) = k^2 - \mu + \frac{1}{2\pi} \int_{-\Lambda}^{+\Lambda} d\lambda \varepsilon(\lambda) K(k, \lambda) \tag{36}$$

Differentiating Eq. (36) with respect to k and taking the integral by parts, we get:

$$\varepsilon'(k) = 2k - \frac{1}{2\pi}\int_{-\Lambda}^{\Lambda} d\lambda \varepsilon'(\lambda) K(k,\lambda) \tag{37}$$

Now, we wish to calculate the energy difference $\Delta E\left(k_p\right)$ between the N - particle ground state and $N+1$ - particle excited state. It is obtained by:

$$\Delta E\left(k_p\right) = k_p^2 - \mu + \sum_{j=1}^{N}\left(\tilde{k}_j^2 - k_j^2\right) = k_p^2 - \mu - \sum_{j=1}^{N} 2k_j\left(k_j - \tilde{k}_j\right) \to k_p^2 - \mu - \int_{-\Lambda}^{\Lambda} dk 2kJ\left(k,k_p\right) \tag{38}$$

Similarly to what we did with the momentum, we multiply Eq. (37) by $-J\left(k,k_p\right)$, integrate over k, and using Eq. (31), we get the identify:

$$2\int_{-\Lambda}^{\Lambda} kJ\left(k,k_p\right)dk = -\frac{1}{2\pi}\int_{-\Lambda}^{\Lambda} d\lambda \varepsilon(\lambda) K\left(k_p,\lambda\right) \tag{39}$$

Substituting Eq. (39) into Eq. (38), we obtain:

$$\Delta E\left(k_p\right) = \varepsilon\left(k_p\right), \quad \left|k_p\right| \geq \Lambda \tag{40}$$

Thus we see the physical meaning of $\varepsilon(k)$ introduced by Eq. (36). It can be interpreted as the energy of an excitation with momentum $p(k)$.

In addition, hole - type excitations can be regarded as excitations generated by the removal of one or more particles from the N - particle ground state. Similarly to what we did above, it can be shown that for one and multiple particle hole excitations respectively, the momentum and energy differences are:

$$\Delta P(k_h) = -p(k_h), \quad -\Lambda \leq k_h \leq \Lambda \tag{41}$$

$$\Delta E(k_h) = -\varepsilon(k_h), \quad -\Lambda \leq k_h \leq \Lambda \tag{42}$$

Therefore, as we add particles with $|k_p| \geq \Lambda$ and holes with $|\lambda_h| \leq \Lambda$ to the system, the total change in energy and momentum is:

$$\Delta P = \sum_{particles} p(k_p) - \sum_{holes} p(k_h) \tag{43}$$

$$\Delta E = \sum_{particles} \varepsilon(k_p) - \sum_{holes} \varepsilon(k_h) \tag{44}$$

Furthermore, we take advantage of the microscopic definition of the Fermi velocity as the derivative of the dressed energy by the dressed momentum at the point where the rapidity equals the Fermi momentum:

$$v_s = \frac{\partial\varepsilon(k)}{\partial p(k)}|_{k=\Lambda} = \left(\frac{\partial\varepsilon(k)}{\partial k}\right) / \left(\frac{\partial p(k)}{\partial k}\right)|_{k=\Lambda} \tag{45}$$

The dressed functions (13) and (36) respectively satisfy the dressing equation with the bare quantity as a source. Now if we add the dressed momentum (32) to the mix, we notice:

$$\frac{\partial p(k)}{\partial k} = 2\pi\rho(k) \tag{46}$$

Thus the sound velocity (or effective velocity of excitations is):

$$v_s = \frac{1}{2\pi\rho(\Lambda)} \frac{\partial\varepsilon(k)}{\partial k}|_{k=\Lambda} \tag{47}$$

2.8 Bogoliubov and the model's spectrum

In the strong coupling limit $\gamma \to \infty$ (TG), we discussed about the fermionization of the 1D Lieb Liniger Bose gas. We saw that the energy spectrum of the model matches that of a single-component noninteracting Fermi gas. However, the problem that arises is the difficulty of describing this Fermi spectrum in boson terms.

The conventional Fermi spectrum is described by regarding the elementary excitation process of taking one particle from one state $q(|q| < \Lambda)$ to another state $k(|k| > \Lambda)$. The respective energy and momentum of this excitation is $\varepsilon(k,q) = k^2 - q^2, p(k,q) = k - q$. So to start, we need two parameters to describe every excitation, contrary to the single parameter we normally use for the Bose case, and thus there is no $\varepsilon(p)$ unique curve. To work around this, two different types of one parameter excitations can be defined:

Type I,"Particle" Excitations . We take a particle from Λ to $q > \Lambda$ or, alternatively, from -Λ to $q < -\Lambda$. This gives an energy and momentum spectrum:

$$\begin{aligned}
&\varepsilon_1 = q^2 - \Lambda^2 \\
&p = q - \Lambda, q > \Lambda \quad \text{or} \quad p = q + \Lambda, q < -\Lambda \\
&\varepsilon_1(p) = p^2 + 2\pi n|p|
\end{aligned}$$

Type II,"Hole" Excitations . We take a particle from $0 < q < \Lambda$ to $\Lambda + \frac{2\pi}{L}$ or, alternatively, from -$\Lambda < q < 0$ to $-\Lambda - \frac{2\pi}{L}$. This gives an energy and momentum spectrum:

$$\begin{aligned}
&\varepsilon_2 = \Lambda^2 - q^2 \\
&p = \Lambda - q, 0 < q < \Lambda \quad \text{or} \quad p = -\Lambda - q, 0 > q > -\Lambda \\
&\varepsilon_2(p) = 2\pi n|p| - p^2
\end{aligned}$$

Below, we present a graph depicting numerical calculations relation to Bogoliubov's theory, made by Lieb-Liniger [3].

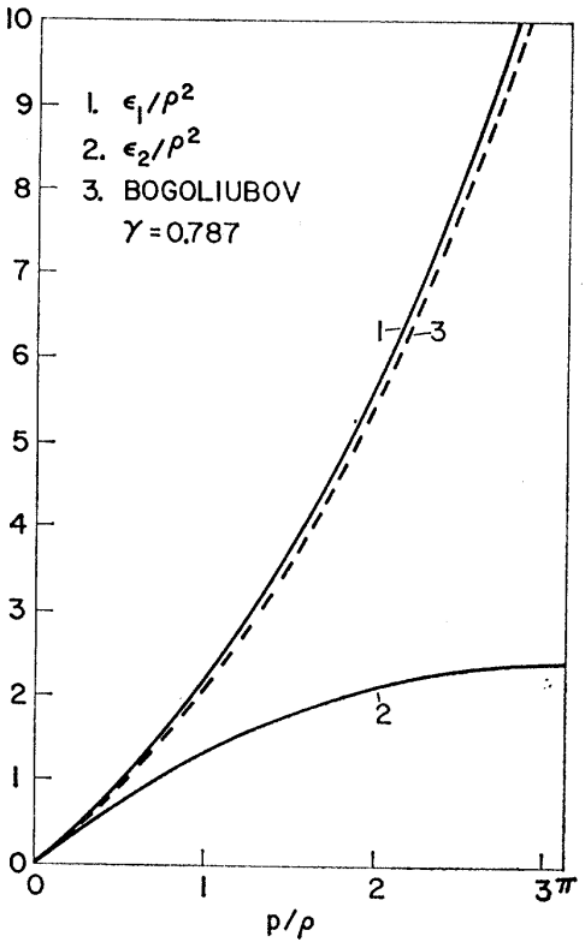

In the figure, we see the excitation spectrum of the Lieb-Liniger model for $\gamma = 0.787$. The vertical axis is dressed energy $\varepsilon(p)/(\hbar^2 n^2 2m)$. *Type I* excitations show a linear dispersion at momenta lower than n and have parabolic-like dispersion at higher momenta, as predicted by Bogoliubov's theory. In contrast, *Type II* excitations, while also showing a linear dispersion at low momenta, behave quite differently at higher momenta. The curve bends down, eventually reaching 0. Finally, it is of value to comment on Lieb-Liniger's [2] comparison to Bogoliubov's theory about the actual numerical values of γ, and what is considered weak, intermediate or strong interaction. In their aforementioned work, they note that the weak interaction regime stands for $\gamma \leq 2$, the intermediate interaction regime for $2 < \gamma < 37$, while the strong interaction regime stands for $\gamma \geq 37$ compared to Bogoliubov's theory, but it is seen, that even for $\gamma = 10$ the large γ approximations are accurate to 1%.

3 Yang-Yang thermodynamics

We now wish to study the system at finite temperatures. To do so, we must consider general excited states. As each eigenstate of the system is characterized by a set of Bethe numbers $\{I_j\}$,the finite-temperature partition function is:

$$\mathcal{Z} = \frac{1}{N!}\sum_{\{I_j\}} e^{-\frac{E_N}{T}} = \sum_{I_1<I_2<\ldots<I_N} e^{-\frac{E_N}{T}} = \sum_{n_1=1}^{\infty}\sum_{n_2=1}^{\infty}\cdots\sum_{n_{N-1}=1}^{\infty} e^{-E_N/T} \tag{48}$$

where $E_N = \sum_{j=1}^{N} k_j^2$. The rapidities k_j are solutions of BA equations (3) with the given set of quantum numbers I_j. Since it is not easy to calculate the energy of a state directly from its quantum numbers, we convert the sums into functional integrals over rapidity densities, at the cost of losing some microscopic information. This loss however is customary in any thermodynamic approach.

Let us also introduce the counting function $y(k)$, that makes the connection clear between the density of quasi-momenta and the corresponding quantum numbers:

$$y(k) \equiv k + \frac{1}{L}\sum_{j=1}^{N}\theta\left(k-k_j\right) \tag{49}$$

By definition, $y\left(k_j\right) = \frac{2\pi}{L}I_j$. There exist other values of k for which the counting function assumes the value $\frac{2\pi}{L}n$ for some n, (half-)integer as for the I_j. These k_n are known as vacancies:

$$y\left(k_n\right) = \frac{2\pi}{L}n \tag{50}$$

Vacancies are "placeholders" for the quantum numbers. Each quantum number n is mapped by the counting function (49) into a k_n. The subset $\left\{k_j^p\right\}$ of vacancies that correspond to the Bethe numbers of the the state are the particles. The remaining solutions $\left\{k_j^h\right\} = \{k_n\}\ \left\{k_j^p\right\}$ are holes, the images of the missing quantum numbers. Considering a state generated from the ground states by removing some quantum numbers from inside the "pseudo" Fermi sphere, those k are the holes.

Now, we define the rapidity densities for the particles, holes and vacancies the same way as in Eq. (8) in the thermodynamic limit :

$$\rho^p\left(k_j^p\right) = \lim_{N,L\to\infty}\frac{1}{L\left(k_{j+1}^p - k_j^p\right)},\quad \rho^h\left(k_j^h\right) = \lim_{N,L\to\infty}\frac{1}{L\left(k_{j+1}^h - k_j^h\right)},\quad \rho\left(k_j\right) = \lim_{N,L\to\infty}\frac{1}{L\left(k_{j+1}-k_j\right)}, \tag{51}$$

Since $L\rho^p(k)dk$ and $L\rho^h(k)dk$ are the number of particles and holes in dk, we have:

$$L\rho(k)dk = L\left[\rho^p(k)+\rho^h(k)\right]dk. \tag{52}$$

It is also easy to prove that:

$$y'\left(k_j\right) = \lim_{N,L\to\infty}\frac{y\left(k_j\right)-y\left(k_{j-1}\right)}{k_j-k_{j-1}} = \lim_{N,L\to\infty}\frac{2\pi}{L\left(k_j-k_{j-1}\right)} = 2\pi\rho\left(k_j\right) \tag{53}$$

Therefore:

$$y(k) = 2\pi\int^{k} d\lambda\left[\rho^p\left(\lambda\right)+\rho^h\left(\lambda\right)\right] \tag{54}$$

Now, we can take the thermodynamic limit of the counting function (49):

$$y(k) = k + \int_{-\infty}^{\infty} d\lambda \rho^p(\lambda)\theta(k-\lambda) \tag{55}$$

along with Eq. (54), equate their RHS and take their derivative with respect to k, to get:

$$\rho^p + \rho^h = \frac{1}{2\pi} + \frac{1}{2\pi}\int_{-\infty}^{\infty} d\lambda K(k-\lambda)\rho^p(\lambda) \tag{56}$$

In contrast with Eq. (13), the introduction of hole density allows the integral to extend over the whole real axis. Compared to that case, this integral is not closed since $\rho^p(k)$ depends on $\rho^h(k)$, which we have not yet determined. In addition, due to the partitions of particles and holes in a small interval dk, the energy of a macroscopic state is degenerate. Such degeneracies give non-zero entropy. The number of microscopic states in dk is:

$$dW = \frac{(L(\rho^p + \rho^h)dk)!}{(L\rho^p dk)!(L\rho^h dk)!} \tag{57}$$

Using Stirling's approximation, Yang and Yang gave the expression for the entropy per unit length:

$$S = \int_{-\infty}^{\infty} dk \left[(\rho^p + \rho^h)\ln(\rho^p + \rho^h) - \rho^p \ln\rho^p - \rho^h \ln\rho^h\right] = \int_{-\infty}^{\infty} dk \left[(\rho^p + \rho^h)\ln\left(1 + \frac{\rho^p}{\rho^h}\right) - \rho^p \ln\left(\frac{\rho^p}{\rho^h}\right)\right] \tag{58}$$

In the grand canonical ensemble, the Gibbs free energy per unit length is $G/L = E/L - \mu n - TS$, where μ is the chemical potential. To determine the true physical state, we need to minimze G with respect to the density of particles and holes, meaning $\delta G/L = \delta E/L - \mu\delta n - T\delta S = 0$. The energy and density per unit length are given in this case by:

$$\frac{E}{L} = \int_{-\infty}^{\infty} k^2 \rho^p(k)dk, \quad \frac{n}{L} = \int_{-\infty}^{\infty} \rho^p(k)dk \tag{59}$$

Applying the infinitesimal variation to the entropy (58) we get:

$$\delta S = \int_{-\infty}^{\infty} dk \left[(\delta^p + \delta\rho^h)\ln\left(1 + \frac{\rho^p}{\rho^h}\right) - \delta\rho^p \ln\left(\frac{\rho^p}{\rho^h}\right)\right] \tag{60}$$

Here the densities are obviously co-dependant, as can be seen by taking the infinitesimal variations of Eq. (56):

$$\delta\rho^p + \delta\rho^h = \frac{1}{2\pi}\int_{-\infty}^{\infty} d\lambda K(k-\lambda)\delta\rho^p(\lambda) \tag{61}$$

Using these relations along with the minimization condition $\delta G/L = 0$, we arrive at:

$$k^2 - \mu - T\ln\left(\frac{\rho^p}{\rho^h}\right) - \frac{Tc}{\pi}\int_{-\infty}^{\infty} \frac{d\lambda}{c^2 + (k-\lambda)^2}\ln\left(1 + \frac{\rho^p}{\rho^h}\right) = 0. \tag{62}$$

Now, by introducing the dressed energy of the system $e^{\varepsilon(k)/T} = \rho^h/\rho^p$, Yang and Yang obtained the now well-known Yang-Yang thermodynamic Bethe Ansatz equation [7]:

$$\varepsilon(k) = k^2 - \mu - T\int_{-\infty}^{\infty} \frac{d\lambda}{2\pi} \frac{2c}{c^2 + (k-\lambda)^2} \ln(1 + e^{-\beta\varepsilon(\lambda)}) \tag{63}$$

through which we can determine the thermodynamics of the system in a whole temperature regime.

In addition, we can derive the pressure in a similar manner through the Bethe Ansatz equations and the relation $P = -\left(\partial G/\partial L\right)_{T,\mu,c}$, which leads to:

$$P = \frac{T}{2\pi}\int_{-\infty}^{\infty} dk \ln(1 + e^{-\beta\varepsilon(k)}) \tag{64}$$

We can then derive various thermodynamic quantities from the pressure, such as density, entropy, compressibility and specific heat:

$$n = \left(\frac{\partial P}{\partial \mu}\right)_{c,T}, \quad S = \left(\frac{\partial P}{\partial T}\right)_{c,\mu}, \quad \varkappa = \left(\frac{\partial^2 P}{\partial \mu^2}\right)_{c,T}, \quad C = \left(T\frac{\partial^2 P}{\partial T^2}\right)_{c,\mu} \tag{65}$$

This approach by Yang and Yang is a powerful method to treating thermodynamics of integrable models, such as those of interacting electrons, spins, fermionic and bosonic atoms. The method has been successfully adapted to treat other models with internal degrees of freedom. We will use Yang and Yang's approach to study the Lieb-Liniger model, in an attempt to obtain its exact thermodynamics.

3.1 Phase Diagram

Before we proceed to discuss the thermodynamics of the Lieb-Liniger model, it is important to see what the phase diagram for the model looks like. We will incorporate two parameters to do so, the dimensionless interaction strength $c = \frac{mc}{n\hbar^2}$ and the dimensionless temperature $t = \frac{\hbar^2 k_B T}{mc^2}$, plotting for the Lieb-Liniger model at thermal equilibrium and discussing, using the phase diagram analysis by [15].

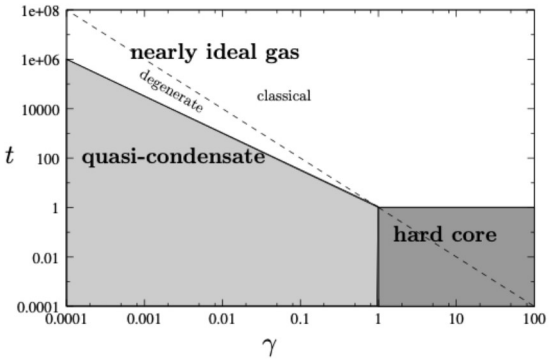

Here, the different asymptotic regimes are separated by smooth crossovers. In ideal Bose gas regime, interactions are negligible. In the quasi-condensate regime, density fluctuations are suppressed due to weak interactions, and the hard-core (TG gas) regime is where fermionization occurs. The crossover between the ideal Bose gas regime and the quasi-condensate regime occurs for $t \simeq \gamma^{-3/2}$. The crossover between the quasi-condensate regime and the hard-core, strongly interacting regime occurs for $\gamma \simeq 1$. Meanwhile, the crossover between the hard-core regime and the ideal Bose gas regime occurs at $t \simeq 1$. The dashed line represents the quantum degeneracy condition, which reads $t \simeq \gamma^{-2}$. An important note is that due to the integrability of the Lieb-Liniger model, thermal equilibrium is not granted.

3.2 Thermodynamics of the Lieb Liniger model

In this section, we proceed to use the relations already establish to get some insight on the thermodynamics of the Lieb Liniger model. In sections **3.1.1** and **3.1.2** we study the low and high temperature limits of the model, respectively. In the low temperature limit, our analytic results of the dressed energy, the chemical potential as well as other thermodynamical quantities are in perfect agreement up to order $\mathcal{O}(\frac{1}{c^2})$ with the analytic results of previous work [13] that has been tested and confirmed numerically. In the high temperature limit, we once again derive the dressed energy and calculate thermodynamical quantities from it in a certain momenta regime, producing results that again match previous confirmed work [11] up to order $\mathcal{O}(\beta^2)$, with identical dependence on important quantities, but difference in some coefficients.

In contrast and perhaps even complimenting previous results, we derive a different analytic approach to calculating various thermodynamical quantities, by asymptotic series expansion in the low temperature limit, and propose that in the high temperature limit one can introduce cutoffs to diverging integrals in order to calculate desired quantities. The fact that our results agree with numerical calculations is a good rule of thumb.

In sections **3.1.3** and **3.1.4** we make a brief review over the weak and strong interaction limits of the model. The weak limit, especially, is an extremely interesting and difficult problem to analytically solve, and we would like to investigate further on it.

3.2.1 Low Temperature $T \to 0$ limit

For starters, it is important to understand the model's behaviour at zero temperature. The TBA Eq. (63) suggests two distinct regimes. One is a vacuum where the chemical potential μ is less than zero, i.e $\mu < \mu_c$, with this model's $\mu_c = 0$ and a filled Fermi sea with bosons of finite density for $\mu > \mu_c$. In the case $\mu = \mu_c = 0$, $\varepsilon(0) = 0$, indicating a phase transition from the vacuum into the Tomonga-Luttinger liquid (TLL) at zero temperature. For $\mu < \mu_c$, and small temperatures, the vacuum becomes populated with an exponentially small number of bosons, meaning that the classical gas phase (CG) persists. For $\mu > \mu_c$, the filled Fermi sea is regarded as the TLL where conformal field theory describes the power-law behavior of correlation functions. In this 1D Lieb-Liniger Bose gas, there is no quantum phase transition, but there exists a crossover temperature T^* below which the TLL with relativistic dispersions can be sustained. Thus, for temperatures $T < T^*$ where T^* separates the TLL from the quantum critical regime (QC), the TLL phase persists.

We will investigate this regime, taking a limit to the zero-temperature case and building on that approximation which has been validated many times, and is the core tool used by other projects to produce numerical results for this model. In the zero-temperature limit after an expansion in temperature T, the Yang-Yang equation (63) can be reduced to [3, 16]:

$$\varepsilon(k) = k^2 - \mu + \int_{-\Lambda}^{+\Lambda} \frac{d\lambda}{2\pi} \frac{2c}{c^2 + (k-\lambda)^2} \varepsilon(\lambda), \quad \varepsilon(\pm\Lambda) = 0, \quad \varepsilon(k) < 0, |k| < \Lambda \tag{66}$$

which is a Fredholm integral equation of the second kind, and can be solved iteratively.

In Eq. (66), Λ, is the integral cut-off for the excited state for single particle excitations, with a gap equal to 2Λ. The restriction $|k| < \Lambda$ places the pseudo-momenta k within the regime dictated by the gap, while the cut-off momenta Λ provide the fermi momentum values $\Lambda = k_F = \pi n$. In literature, one finds common use of the parameter γ to associate cut-off and interaction strength c. With our convention, we relate these parameters by $\gamma = \frac{\pi c}{\Lambda}$, $\gamma = \frac{c}{n}$, where $n = \frac{N}{L}$ is the number density of the particle species that undergo excitation .

To proceed with the solution of Eq. (66), let $\phi(k) = k^2 - \mu$. Then, the equation becomes:

$$\varepsilon(k) = \phi(k) + \frac{c}{\pi} \int_{-\Lambda}^{+\Lambda} d\lambda \frac{1}{c^2 + (k-\lambda)^2} \varepsilon(\lambda) \tag{67}$$

Using a Liouville-Neumann series, the iterated kernel is:

$$K_1(k) = \frac{1}{1 + (k/c)^2}. \tag{68}$$

We can re-write the n -th iterated kernel as:

$$K_n(k, \lambda) = \left(\prod_{i=1}^{n-1} \int_{-\Lambda}^{\Lambda} dq_i \right) K_1(k - q_1) K_1(q_1 - q_2) \dots K_1(q_{n-1} - \lambda) \tag{69}$$

Then, the resolvent is given by:

$$R(k, \lambda) = \sum_{n=1}^{\infty} \left(\frac{1}{\pi c} \right)^n K_n(k, \lambda) \tag{70}$$

and the solution of Eq. (67) is given by:

$$\varepsilon(k) = k^2 - \mu + \int_{-\Lambda}^{+\Lambda} R(k, \lambda) \phi(\lambda) d\lambda \tag{71}$$

This expression provides us with a perturbative series, which is a natural starting point to start calculating corrections to the dressed energy $\varepsilon(k)$. The zeroth order ($\pi c = \infty$) hardcore limit provides of course the expected result $\varepsilon(k)|_{c=\infty} = k^2 - \mu^2$. In this case, we can already see that the chemical potential μ, must satisfy the relation $\mu = \Lambda^2$, where Λ is the exact momentum of excitations at which the dispersion relation $\varepsilon(k)|_{c=\infty}$ changes sign.

It is now important to discuss the Tonks-Girardeau gas regime. In this section, considering low temperatures and the state of the model dominated by the interaction strength, as is evident (assuming repulsive interactions), the Lieb-Liniger bosons behave like ideal particles obeying fractional statistics. We could press on this matter to calculate local two-particle correlation functions for the model, but it does not concern our work directly. In this regime, we can safely use the fact $c \gg 1$ to make approximations and continue our calculations.

Now, since the properties of the model are dominated by the interaction strength we expand the series to first order in $\frac{1}{\pi c}$ as well as integrate over λ to obtain:

$$\begin{aligned}\varepsilon(k) = (k^2 - \mu)\left[1 + \frac{1}{\pi}\left\{\arctan\left(\frac{\Lambda + k}{c}\right) + \arctan\left(\frac{\Lambda - k}{c}\right)\right\}\right] \\ + \frac{c^2}{\pi}\left[\frac{2\Lambda}{c} - \arctan\left(\frac{\Lambda + k}{c}\right) - \arctan\left(\frac{\Lambda - k}{c}\right)\right] + \frac{ck}{\pi}\ln\left(\frac{|c^2 + (\Lambda - k)^2|}{|c^2 + (\Lambda + k)^2|}\right) + \mathcal{O}\left(\frac{1}{c^2}\right)\end{aligned} \tag{72}$$

Next, assuming small momentum and finite particle density such that $\frac{k}{c} \ll 1, \frac{\Lambda}{c} \ll 1$ (i.e. the strong coupling limit) we can expand Eq. (75) to obtain:

$$\boxed{\varepsilon(k) = k^2 - \mu\left(1 + \frac{2\Lambda}{\pi c}\right) + \frac{2\Lambda^3}{3\pi c} + \mathcal{O}\left(\frac{1}{c^2}\right)} \tag{73}$$

Notice that Eq. (73) can be obtained directly from a perturbative expansion of Eq. (67), by expanding the integral kernel $\frac{1}{c^2 + (k-\lambda)^2}$ as a series around $\frac{1}{\pi c}$ and neglecting all orders except first, provided of course that $\frac{\Lambda}{c} \ll 1$. This implies that the effective mass m_{eff} is unchanged to second order expansion, since we can re-write equation (73) as $\varepsilon(k) = k^2 - \mu\left(1 + \frac{4\Lambda}{3\pi c}\right) + \mathcal{O}\left(\frac{1}{c^2}\right) = \frac{k_F^2}{2m_{\text{eff}}} + E_0$, utilizing the powerful relation $\mu \approx \Lambda^2 = k_F^2$. Of course, our solution provides us the ability to calculate higher order corrections if we so wish, but performing the calculations is beyond the scope of this project.

In addition, utilizing the fact that $\varepsilon(\pm\Lambda) = 0$, we can derive a first order in $\frac{1}{\pi c}$ relation for the chemical potential:

$$\boxed{\mu(\Lambda) = \Lambda^2\left[1 - \frac{4\Lambda}{3\pi c}\right] + \mathcal{O}\left(\frac{1}{c^2}\right)} \tag{74}$$

One can notice that Eq. (74) is an interesting case, but for our study we will approximate $\mu \approx \Lambda^2$.

Let us discuss over the implications of our results for the dressed energy $\varepsilon(k)$, through which many thermodynamic properties of the model follow. In Figure 1, we present a comparison between our solution for Eq. (67) and the strong coupling expansion (73), as well as the hardcore limit $c = \infty$, choosing parameters $\mu = 3$, $c = 10$. In the figure, we can see that for small momenta the dressed energy is significantly renormalized from the hardcore limit when we use our approximation $\mu = \Lambda^2$. For larger momenta not shown in the plot, the dressed energy $\varepsilon(k)$ retains its parabolic shape and is close to the $c = \infty$ limit. Thus, we can see that our results are a very good approximation for the regime $k \in [-\Lambda, \Lambda]$. Before proceeding to further evaluations, we provide a conversion of our solution for the dressed energy $\varepsilon(k)$ as well as the approximation for the chemical potential μ using the common γ parameter:

$$\varepsilon(k) = k^2 - \pi^2 n^2 \left(1 + \frac{4}{3\gamma}\right) + \mathcal{O}\left(\gamma^{-2}\right)$$
$$\mu(\Lambda) = \pi^2 n^2 \left(1 - \frac{4}{3\gamma}\right) + \mathcal{O}\left(\gamma^{-2}\right)$$

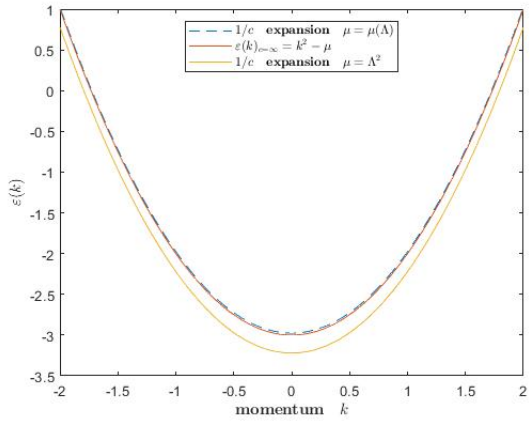

Figure 2: Dressed Energy $\varepsilon(k)$ as a function of momentum k for $\Lambda = \sqrt{3}, c = 10$.

Now, we proceed to evaluate the derivative of the dressed momentum with respect to the bare momenta. It is given by:

$$\frac{dp}{dk} = 1 + \int_{-\Lambda}^{+\Lambda} \frac{2c}{c^2 + (k-\lambda)^2} n(\lambda) \frac{dp}{d\lambda} \frac{d\lambda}{2\pi} \tag{75}$$

Since we know (66) that $\varepsilon(k) < 0$, we can re-write $n(\lambda)$ in the low temperature limit:

$$\lim_{\beta\to\infty} n(\lambda) = \lim_{\beta\to\infty} \frac{1}{1 + e^{\beta\varepsilon_\lambda}} = \lim_{\beta\to\infty} \frac{1}{1 + \frac{1}{e^{-\beta\varepsilon_\lambda}}} = 1 \tag{76}$$

Now, using the same iterated kernel (68) and resolvent (70), by letting $\phi(\lambda) = 1$, we obtain:

$$\frac{dp}{dk} = 1 + \int_{-\Lambda}^{+\Lambda} R\left(k, \lambda, \frac{c}{\pi}\right) \phi(\lambda) d\lambda \tag{77}$$

which, after expanding the resolvent to first order and performing the integration over λ gives:

$$\frac{dp}{dk} = 1 + \frac{1}{\pi}\left[\arctan\left(\frac{\Lambda + k}{c}\right) + \arctan\left(\frac{\Lambda - k}{c}\right)\right] \tag{78}$$

In the strong coupling limit of the TG gas, Eq. (78) simplifies to:

$$\frac{dp}{dk} = 1 + \frac{2\Lambda}{\pi c} + \mathcal{O}\left(\frac{1}{c^2}\right) \tag{79}$$

We can integrate Eq. (79) over k and use the fact that at the limit $c \to \infty$, $p(k) = k$, to obtain:

$$\boxed{p(k) = k\left(1 + \frac{2\Lambda}{\pi c}\right) + \mathcal{O}\left(\frac{1}{c^2}\right)} \tag{80}$$

Solving Eq. (80) with respect to k and substituting into Eq. (73) gives:

$$\boxed{\varepsilon(p) = p^2\left(1 - \frac{4\Lambda}{\pi c}\right) - \mu\left(1 + \frac{2\Lambda}{\pi c}\right) + \frac{2\Lambda^3}{3\pi c} + \mathcal{O}\left(\frac{1}{c^2}\right)} \tag{81}$$

where of course we have taken the denominator $\frac{1}{1+\frac{2\Lambda}{\pi c}} \approx 1 - \frac{2\Lambda}{\pi c} + \mathcal{O}\left(\frac{1}{c^2}\right)$.

In Eq. (81), it is evident that the dressed energy $\varepsilon(p)$ is also renormalized when concerning its dependance on real and not-quasi momenta.

Now, putting our results to good use, we can calculate the sound velocity through the relation:

$$v_s = \frac{\partial\varepsilon(k)}{\partial p(k)}|_{k=\Lambda} \tag{82}$$

Solving, we obtain (in perfect agreement with [11] up to first order in c):

$$\boxed{v_s = 2\Lambda\left(1 - \frac{4\Lambda}{\pi c}\right) + \mathcal{O}\left(\frac{1}{c^2}\right) = 2\pi n\left(1 - \frac{4}{\gamma}\right) + \mathcal{O}\left(\gamma^{-2}\right)} \tag{83}$$

In the $T \to 0$ limit, the Gibbs free energy density is given by:

$$g = \frac{-T}{2\pi}\int_{-\Lambda}^{+\Lambda} dk \ln(1 + e^{-\beta\varepsilon(k)}) \approx \frac{1}{2\pi}\int_{-\Lambda}^{+\Lambda} dk\varepsilon(k) \tag{84}$$

Substituting the dressed energy from Eq. (73) and taking $\Lambda^2 = \mu$, we obtain:

$$\boxed{g = -\left[\frac{2\mu^{3/2}}{3\pi} + \frac{4\mu^2}{3\pi^2 c}\right] + \mathcal{O}\left(\frac{1}{c^2}\right) = -\frac{2\pi^2 n^3}{3}\left(1 + \frac{2}{\gamma}\right) + \mathcal{O}\left(\gamma^{-2}\right)} \tag{85}$$

Deriving the Gibbs free energy allows us to calculate thermodynamic properties of the model.

This result is powerful, as it allows us to continue expanding Eq. (72) in higher orders of $\frac{1}{c}$ and witness the model's corrections. We will discuss this more in the $c \to \infty$ section.

The pressure is $P = -g = \frac{1}{2\pi}\int_{-\Lambda}^{+\Lambda} dk\varepsilon(k)$, and thus we obtain the compressibility:

$$\boxed{\varkappa = -\frac{\partial^2 g}{\partial\mu^2} = \frac{\mu^{-1/2}}{2\pi} + \frac{8}{3\pi^2 c} + \mathcal{O}\left(\frac{1}{c^2}\right) = \frac{1}{2\pi^2 n}\left(1 + \frac{16}{3\gamma}\right) + \mathcal{O}\left(\gamma^{-2}\right)} \tag{86}$$

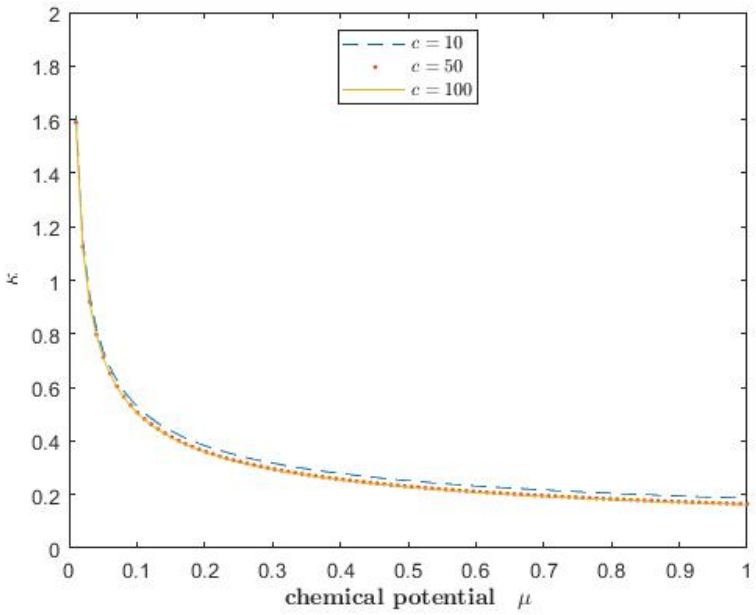

Figure 3: Compressibility $\varkappa$ as a function of the chemical potential μ for varying values of the interaction strength c.

3.2.2 High temperature $\beta \to 0$ limit

Expanding the logarithmic term inside the Yang-Yang equation (63) at $\beta \to 0$ to first order, we obtain:

$$\varepsilon(k) = k^2 - \mu - T\int_{-\infty}^{+\infty} \frac{d\lambda}{2\pi} \frac{2c}{c^2 + (k-\lambda)^2} \left[\ln(2) - \frac{1}{2}\beta\varepsilon(\lambda)\right] \tag{87}$$

and after performing the first integral:

$$\varepsilon(k) = k^2 - \mu - \ln(2)T + \frac{c}{2\pi}\int_{-\infty}^{+\infty} d\lambda \frac{1}{c^2 + (k-\lambda)^2}\varepsilon(\lambda) \tag{88}$$

The following calculations assume a finite, small interaction strength c. Now, using the convolution theorem for the kernel (68) and dressed energy, we proceed to Fourier transform Eq. (88):

$$\varepsilon(k) = k^2 - \mu - \ln(2)T + \frac{c}{2\pi}K \circ \varepsilon(k) \Rightarrow \varepsilon(\omega) = -2\pi\delta''(\omega) - 2\pi\left[\mu + \ln(2)T\right]\delta(\omega) + \frac{c}{2\pi}K(\omega)\varepsilon(\omega) \tag{89}$$

Additionally, we have that:

$$K(\omega) = \int_{-\infty}^{+\infty} dk \frac{e^{-i\omega k}}{c^2 + k^2} = \frac{\pi}{c}e^{-c|\omega|} \tag{90}$$

$$\int_{-\infty}^{+\infty} d\omega \delta^{(n)}(\omega - \alpha) f(\omega) = f^{(n)}(\alpha) \tag{91}$$

$$\varepsilon(\omega) = -2\pi\delta''(\omega) - 2\pi\left[\mu + \ln(2)T\right]\delta(\omega) + \frac{1}{2}e^{-c|\omega|}\varepsilon(\omega) \Rightarrow \varepsilon(\omega)\left(1 - \frac{e^{-c|\omega|}}{2}\right) = -2\pi\delta''(\omega) - 2\pi\left[\mu + \ln(2)T\right]\delta(\omega) \tag{92}$$

$$\varepsilon(\omega) = -4\pi\left[\frac{\delta''(\omega) + \left[\mu + \ln(2)T\right]\delta(\omega)}{2 - e^{-c|\omega|}}\right] \tag{93}$$

After straight forward calculations, we inverse the Fourier transform. Hence, up to first order in β:

$$\boxed{\varepsilon(k) = k^2 - 3c^2 - \frac{\mu}{2} - \frac{\ln(2)}{2}T + \mathcal{O}(\beta^2)} \tag{94}$$

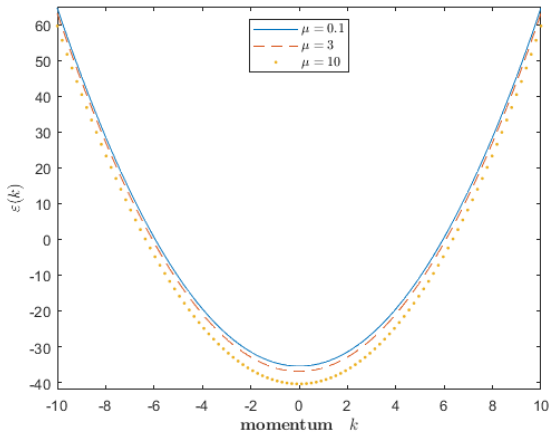

Figure 4: Dressed Energy $\varepsilon(k)$ as a function of momentum k for T=100, c=0.5.

Now, we calculate the free energy density the same way as in the low temperature limit. We place a cutoff Q at the integral, Q playing the role of the upper and lower boundary of the available momenta to the system, given the fact that we wish to restrict the available momenta to certain values, as dictated by the high temperature limit. After expanding around $\beta \to 0$ in the integral and keeping terms up to first order in β, we get:

$$\boxed{g = -\frac{T}{2\pi}\int_{-Q}^{Q} dk \ln\left(1 + e^{-\beta\varepsilon(k)}\right) = -\frac{\mu^{1/2}}{\pi}\left[\frac{3}{2}c^2 + \frac{\mu}{12} + \frac{5}{4}T\ln(2)\right] + \mathcal{O}(\beta^2)} \tag{95}$$

where we have once again approximated $\mu \approx Q^2$. A Virial expansion with the Yang-Yang equation (63) was considered by [11]. Up to second Virial coefficient, the result they obtained for the pressure P was:

$$P = P_0 + \frac{T^{3/2}}{\sqrt{2\pi}}\mathcal{Z}^2 P_2 \tag{96}$$

where $\mathcal{Z} = e^{\mu/T}$ is the fugacity, $P_2 = -\frac{1}{2} + \int_{\infty}^{\infty} dk K(2k) e^{-2k^2/T}$ reveals the two-body interaction effect and $P_0 = -\frac{T}{2\pi}\int_{\infty}^{\infty} dk \ln(1 - \mathcal{Z}e^{-k^2/T})$ is the pressure of the free bosons. We have also considered this solution and we plot it along our solution for the pressure in Figure 6.

Now we proceed to calculate the compressibility in the high temperature limit from Eq. (95):

$$\boxed{\varkappa = -\frac{\partial^2 g}{\partial \mu^2} = \frac{\mu^{-1/2}}{16\pi} - \frac{5T\ln(2)\mu^{-3/2}}{16\pi} - \frac{3c^2\mu^{-3/2}}{8\pi} + \mathcal{O}(\beta^2)} \tag{97}$$

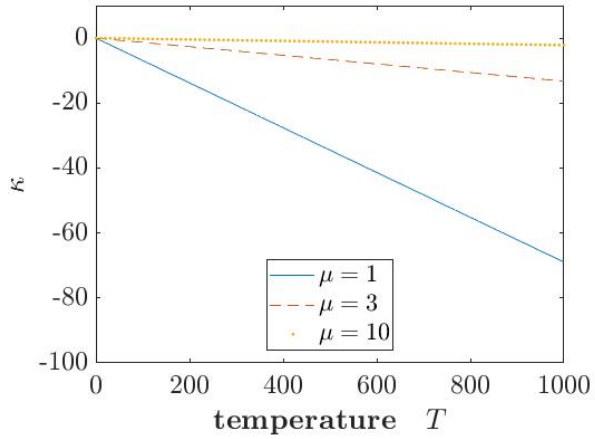

Figure 5: Compressibility $\varkappa$ as a function of Temperature T for varying values of the chemical potential μ and c =0.5

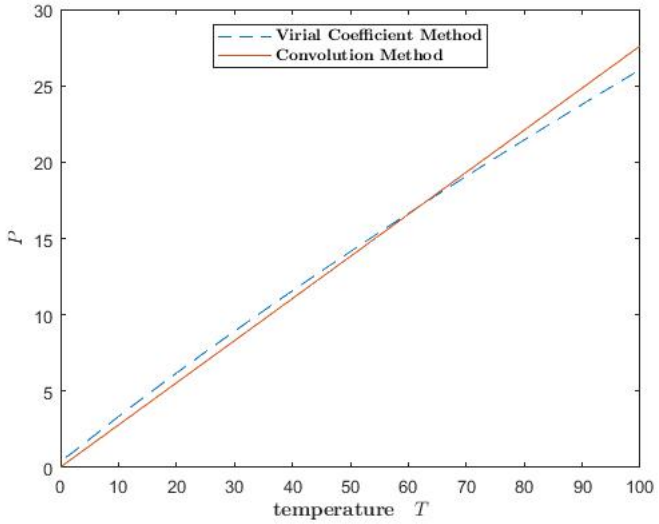

Figure 6: Pressure P as a function of temperature. We compare our asymptotic series method with the Virial coefficient method of [11] for $\mu = 1, c = 0.1$.

3.2.3 Weak Interaction $c \to 0^+$ limit

In the weak coupling limit, the system should have the behaviour of free bosons. In this weak coupling limit, we observe for the kernel :

$$\lim_{c\to 0^+} K(k,\lambda) = \lim_{c\to 0^+} \frac{c/\pi}{c^2+(k-\lambda)^2} = \delta(k-\lambda) \tag{98}$$

Therefore, the dressed energy (63) becomes:

$$\varepsilon(k) = T\ln\left(e^{\beta(k^2-\mu)}-1\right) \tag{99}$$

Using Eq. (99) along with Eq. (56), we obtain:

$$2\pi\rho^p(k) = e^{-\beta\varepsilon(k)} = \frac{1}{e^{\beta(k^2-\mu)}-1}, \tag{100}$$

which is exactly the distribution function for free bosons.

Then, the pressure is given by:

$$P = \frac{T}{2\pi}\int_{-\infty}^{\infty} \ln\left(1-e^{-\beta(k^2-\mu)}\right) \tag{101}$$

3.2.4 Strong Interaction $c \to \infty$ limit

In the strong coupling limit, the kernel vanishes and therefore the dressed energy (63) becomes:

$$\varepsilon(k) = k^2-\mu \tag{102}$$

Using Eq. (102) along with Eq. (56), we obtain:

$$2\pi\rho^p(k) = e^{-\beta\varepsilon(k)} = \frac{1}{e^{\beta(k^2-\mu)}+1}, \tag{103}$$

which is exactly the distribution function for free electrons.

Here, the pressure is given by:

$$P = \frac{T}{2\pi}\int_{-\infty}^{\infty} \ln\left(1+e^{-\beta(k^2-\mu)}\right) \tag{104}$$

In Figure 7, we compare our zero-temperature limit result for the pressure with Peng, Yu and Guan [17] calculations for strong coupling and low temperatures, which is also based on the work of [13].Below we present the polylogarithmic function solution for the pressure P, derived by [13], followed by the series expansion solution of [17], up to order $\mathcal{O}\left(T^4, \frac{1}{c^3}\right)$:

$$P = -\frac{1}{2\sqrt{\pi}}T^{3/2}\mathrm{Li}_{3/2}\left(-e^{A/T}\right), A = \mu + \frac{2}{c}P. \tag{105}$$

$$P \approx \frac{2}{3\pi}\mu^{3/2} + \frac{4}{3\pi^2 c}\mu^2 + \frac{28}{9\pi^3 c^2}\mu^{5/2} + T^2\left(\frac{\pi}{12}\mu^{-1/2} + \frac{1}{9c} + \frac{5}{18\pi c^2}\mu^{1/2}\right). \tag{106}$$

It is obvious that Eq. (82) converted to pressure via $P = -g$ is identical to Eq. (101), up to $\mathcal{O}(\frac{1}{c^2})$. Our results further converge with the polylogarithmic function solution in this regime if we keep higher orders in the expansion of the dressed energy (72).

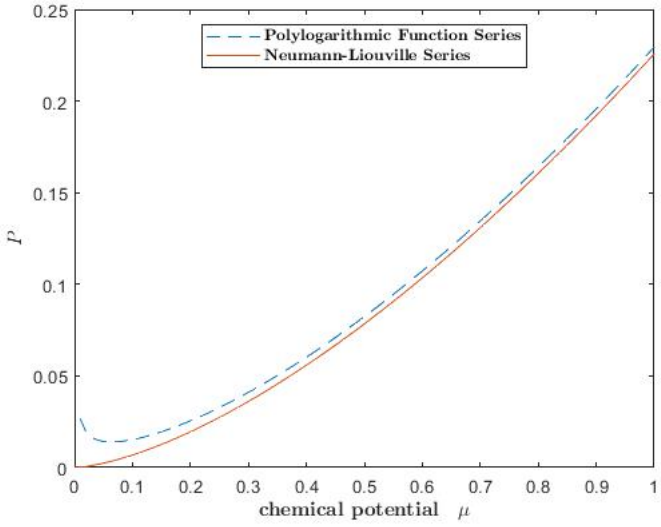

Figure 7: Pressure P as a function of the chemical potential μ. We compare our method with the polylogarithmic function series expansion result through the calculations of [17] for $T = 0.1, c = 10$.

The cited results achieve numerical compatibility with a Sommerfeld expansion over the dressed energies $\varepsilon(k)$, even providing more accurate results. Our analytic calculations match the cited work, providing relations that can be used quickly without the aid of numerical assumptions, at the cost of some accuracy next to Fermi points. However, since our results are analytical, we are able to calculate errors and compare with possible experimental results. But this is beyond the scope of our work, at the moment.

4 Generalized Hydrodynamics

The term Generalized Hydrodynamics, or GHD, originates from 2016. The word 'Generalized' is used in the same way as it is in the Generalized Gibbs Ensemble; it designates the extension of a concept from the case with a small, finite, number of conserved quantities to the case with infinitely many of them.

In 2016, the Generalized Hydrodynamics equation, which we will show below, appeared in the context of quantum integrable one-dimensional systems. In the decade that preceded this breakthrough, tremendous progress has been made on out-of-equilibrium quantum dynamics, largely driven by advances in cold atom experiments, such as the 2006 Quantum Newton Cradle experiment, where two one-dimensional clouds of interacting atoms in a harmonic potential $V(x)$ undergo thousands of collisions, seemingly escaping convergence towards thermal equilibrium. Between 2006 and 2016, many advances on the thermalization of isolated quantum systems occurred, particularly concerning the Generalized Gibbs Ensemble, yet a quantitatively reliable modeling of the Quantum Newton Cradle setup had remained out of reach. As is usual with quantum many-body systems, the exponential growth of the Hilbert space with the number of atoms N seemingly prevented direct numerical simulations of the dynamics.

However, the 2016 breakthrough of GHD changed this state of affairs. Realizing that the dynamics of one-dimensional ultracold quantum gases in experiments such as the Quantum Newton Cradle is captured by GHD equations has brought forth a new era for their theory description.

In this section, we go over the basic approach for the formulation of the GHD equations for the Lieb-Liniger model, though it is easy to extend the method over other models. Then, we put them to use to derive important quantities, such as the energy and energy current correlators, as well as the thermal Drude weight.

4.1 GHD in the Lieb-Liniger model

In second-quantized form, the Lieb-Liniger Hamiltonian is:

$$\mathcal{H} = \int dx \mathbf{h}(x) = \int dx \left(\frac{1}{2} \partial_x \hat{\Psi}^\dagger \partial_x \hat{\Psi} + c \hat{\Psi}^\dagger \hat{\Psi}^\dagger \hat{\Psi} \hat{\Psi} \right) \tag{107}$$

The Hamiltonian has an infinite number of conserved charges $\hat{Q}_i, i = 0, 1, 2...$, with $\hat{Q}_0$ being the particle number, $\hat{Q}_1$ the total momentum, $\hat{Q}_2$ the total energy and so forth.

Thus:

$$\hat{Q}_i = \int dx \mathbf{q}_i(x) \tag{108}$$

where:

$$\begin{aligned} \mathbf{q}_0(x) &= n(x) = \hat{\Psi}^\dagger(x)\hat{\Psi}(x) \\ \mathbf{q}_1(x) &= p(x) = i\hat{\Psi}^\dagger(x)\partial_x\hat{\Psi}(x) + h.c. \\ \mathbf{q}_2(x) &= \mathbf{h}(x) \end{aligned}$$

We also define the conserved currents $\mathbf{j}_i$ corresponding to conserved charge densities. The currents and densities satisfy the continuity equations:

$$\partial_t \mathbf{q}_i + \partial_x \mathbf{j}_i = 0 \tag{109}$$

The Lieb-Liniger model is an integrable system. Thus, we move, through entropy maximization, to Generalized Gibbs Ensembles (GGE) with (formal) density matrix:

$$\rho_{GGE} = e^{-\sum_i \beta_i \hat{Q}_i} \tag{110}$$

As a result, $\langle e^{i\mathcal{H}t}\hat{\mathcal{O}}e^{-i\mathcal{H}t}\rangle \approx \left[\rho_{GGE}(x,t)\hat{\mathcal{O}}\right]$, where the only space-time dependence is in the density matrix, and:

$$\mathbf{q}_i(x,t) = [\rho_{GGE}(x,t)\mathbf{q}_i(x,t)] \tag{111}$$
$$\mathbf{j}_i(x,t) = [\rho_{GGE}(x,t)\mathbf{j}_i(x,t)] \tag{112}$$

satisfy the same continuity equation (109).

Now, the interactions of the repulsive ($c > 0$) Lieb-Liniger model are described by the differential scattering phase:

$$K(\theta) = \frac{2c}{c^2 + \theta^2}, \tag{113}$$

and each conserved charge is characterized by its one-particle eigenvalue $h_i(\theta) = \theta^i/i!$. In the thermodynamic limit, we express the eigenstates in terms of $\rho_p(x,\theta)dxd\theta$, which are the number of quasi-particles. These lead to current densities $\mathbf{q}_i = \int d\theta \rho_p(\theta)h_i(\theta)$. It is convenient to use the variable $n(\theta) = \rho_p(\theta)/\rho_s(\theta)$, with $n(\theta)$ being the occupation function and $\rho_s(\theta)$ the state density $2\pi\rho_s(\theta) = 1 + \int da K(\theta - a)\rho_p(a)$. Then, the density and current averages take the form:

$$\mathbf{q}_i = \int \frac{dp(\theta)}{2\pi} n(\theta) h_i^{dr}(\theta) \tag{114}$$
$$\mathbf{j}_i = \int \frac{dE(\theta)}{2\pi} n(\theta) h_i^{dr}(\theta) = \int \frac{dp(\theta)}{2\pi} n(\theta) v^{\mathit{eff}}(\theta) h_i^{dr}(\theta) \tag{115}$$

where the dressing operation is defined as:

$$h^{dr}(\theta) = h(\theta) + \int \frac{da}{2\pi} K(\theta - a) n(a) h^{dr}(a) \tag{116}$$

Now, demanding the continuity equation (109) along with the above averages gives the continuity equation for quasi-particle parameter θ:

$$\partial_t n(\theta) + v^{\mathit{eff}}(\theta)\partial_x n(\theta) = 0 \tag{117}$$

where the effective velocity $v^{\mathit{eff}}(\theta)$ is the velocity of elementary excitation:

$$v^{\mathit{eff}}(\theta) = \frac{(E')^{dr}(\theta)}{(p')^{dr}(\theta)} \tag{118}$$

4.2 Calculations

Promoting the particle occupation functions to have space-time dependance, we re-write Eq. (117) as:

$$\partial_t n(x,t;\theta) + v^{\mathit{eff}}(x,t;\theta)\partial_t n(x,t;\theta) \tag{119}$$

We recall the dressed energies for the Lieb-Liniger model (63) in the generalized TBA are:

$$\varepsilon^{dr}(\theta) = \varepsilon(\theta) - \int \frac{da}{2\pi} K(\theta, a) \ln(1 + e^{-\varepsilon^{dr}(a)}), \quad \varepsilon(\theta) = \theta^2 - \mu \tag{120}$$

We can write the mean value of the total energy as:

$$E(\theta) = \int d\theta \rho^p(\theta)\varepsilon(\theta) = \int \frac{dp(\theta)}{2\pi} n(\theta)\varepsilon^{dr}(\theta) = \int \frac{dp^{dr}(\theta)}{2\pi} n(\theta)\varepsilon(\theta) \tag{121}$$

Now, we consider a temperature perturbation $\delta\beta_q e^{iqx}$ around the equilibrium state at inverse temperature β, $n(x,t) = n + \delta n(x,t) = n + \delta n(t)\delta\beta_q e^{iqx}$. Substituting in the continuity equation (119) and suppressing θ for convenience, we obtain:

$$\delta n(x,t) = \left(\frac{\partial n}{\partial \beta}\right)_\beta e^{iq(x-vt)} \tag{122}$$

Then, the space-time dependence of the total energy in Eq. (121) becomes:

$$E(x,t) = \int d\theta r(x,t) n(x,t)\varepsilon = \int d\theta \left(r + \delta r(x,t)\right)\left(n + \delta n(x,t)\right)\varepsilon \Rightarrow E(x,t) = E + \delta E(x,t) \tag{123}$$

After linearization on Eq. (123), as done in [18], we obtain:

$$\delta E(x,t) \approx \int d\theta \left(\delta r(x,t) n + r\delta n(x,t)\right)\varepsilon$$

$$\frac{\delta E(x,t)}{\delta \beta_q} \approx \int d\theta \left(\left(\frac{\partial r}{\partial \beta}\right)_\beta n + r\left(\frac{\partial n}{\partial \beta}\right)_\beta\right)\varepsilon e^{iq(x-vt)}$$

$$\frac{\delta E(x,t)}{\delta \beta_q} \approx -\int \frac{dp^{dr}}{2\pi} n(1-n)\left(\varepsilon^{dr}\right)^2 e^{iq(x-vt)}$$

Taking a Fourier Transform, we obtain:

$$\frac{1}{2\pi}\int dt e^{i\omega t}\frac{\delta E(x,t)}{\delta \beta_q} \approx -\int \frac{dp^{dr}}{2\pi} n(1-n)\left(\varepsilon^{dr}\right)^2 \delta(\omega - qv) e^{iqx} = -S_{EE}(q,\omega)e^{iqx} \tag{124}$$

$$\boxed{S_{EE}(q,\omega) = \int \frac{dp^{dr}}{2\pi} n(1-n)\left(\varepsilon^{dr}\right)^2 \delta(\omega - qv)} \tag{125}$$

This is the energy structure factor within GHD at the $q \to$ limit. It is related to the specific heat $C(T)$in this limit, via $C = \beta^2 \int d\omega S_{EE}(q,\omega)$.

Performing a similar analysis for the energy current, we obtain:

$$\frac{\delta J_E(x,t)}{\delta \beta_q} \approx -\int \frac{dp^{dr}}{2\pi} n(1-n)\varepsilon^{dr} j_E^{dr} e^{iq(x-vt)} \tag{126}$$

It is interesting to observe that the time derivative of Eq. (126) obeys a continuity equation in q-space:

$$\frac{\partial}{\partial t}\frac{\delta J_E(x,t)}{\delta \beta_q} - iq\int \frac{dp^{dr}}{2\pi} n(1-n)\left(j_E^{dr}\right)^2 e^{iq(x-vt)} = 0 \tag{127}$$

with current related to the thermal Drude weight [19]:

$$\boxed{D_{th} = \frac{\beta^2}{2}\int \frac{dp^{dr}}{2\pi} n(1-n)\left(j_E^{dr}\right)^2 = \frac{\beta^2}{2}\int \frac{dp^{dr}}{2\pi} n(1-n)\left(v\varepsilon^{dr}\right)^2} \tag{128}$$

Following the same procedure as we did with the energy, we obtain the energy current-current correlator:

$$\boxed{S_{J_E J_E}(q,\omega) = \int \frac{dp^{dr}}{2\pi} n(1-n)\left(j_E^{dr}\right)^2 \delta(\omega - qv)} \tag{129}$$

To note on the spectrum of $S_{J_E J_E}(q,\omega)$, it essentially looks as a δ-function, as $q \to 0$, with weight D_{th}.

5 Concluding Remarks

In conclusion, we reviewed the basic principles of the Lieb-Liniger model using the Bethe ansatz equations, as well as the basics of Yang-Yang thermodynamics. We investigated the thermodynamic properties of the model in the high and low temperature regimes, for strong and weak interactions respectively. We compared our analytic results with other results, established in literature, and achieved great success in describing the finite temperature dynamics of the model, within the context of this thesis. Furthermore, we reviewed the Generalized Hydrodynamics formalism and derived equations through its basic continuity equation, which, along with our analytic solutions, can be used to obtain a more complete picture of the Lieb-Liniger model.

To evolve and take our work to the next level, we can use our methods in higher precision, by expanding in higher orders. However, this was not necessary here, as we have demonstrated the convergence of our work with already established results. It is note-worthy, that the high temperature regime of the Lieb-Liniger model, as well as the weak interaction regime, has not received adequate attention, mostly due to the sheer difficulty of finding exact solutions. We would like to investigate further these regimes, and also make use of numerical methods to verify our results. Given time and enough effort, we could also obtain analytic expressions for the important GHD quantities we derived. Of course, the methods used here can be applied to other integrable models obeying Bethe ansatz equations, and perhaps this could lead to a better understanding of exactly solvable models.

Acknowledgements

I would like to sincerely offer my gratitude to both my friends, colleagues and family. They have aided and supported me tremendously in the process of writing my thesis. I would also like to express both gratitude and respect to my advisor, Prof. Zotos Xenophon, for his guidance and patience with me as I navigated my first steps in the real work demanded by academic physics.

In addition, I would like to break formalities and pay my humble respect, as well as say farewell to Prof. Tomaras Theodore, who passed away early in summer 2021. He was an excellent professor and mentor, but most importantly, he was a true inspiration to all of us that sought out truths behind the equations. I, as well as many of my friends -which he taught-, and the department of physics in the U.O.C. will miss him dearly, and will strive to meet the challenges and examples he set for us.

References

[1] H. Bethe. Zur theorie der metalle. *Z. Physik*, 71:205, 1931.

[2] Elliott H. Lieb. Exact analysis of an interacting bose gas. ii. the excitation spectrum. *Phys. Rev.*, 130:1616–1624, May 1963.

[3] Elliott H. Lieb and Werner Liniger. Exact analysis of an interacting bose gas. i. the general solution and the ground state. *Phys. Rev.*, 130:1605–1616, May 1963.

[4] C. N. Yang. Some exact results for the many-body problem in one dimension with repulsive delta-function interaction. *Phys. Rev. Lett.*, 19:1312–1315, Dec 1967.

[5] Rodney J Baxter. One-dimensional anisotropic Heisenberg chain. *Annals of Physics*, 70(2):323–337, 1972.

[6] M. Gaudin. Un systeme a une dimension de fermions en interaction. *Physics Letters A*, 24(1):55–56, 1967.

[7] C. N. Yang and C. P. Yang. Thermodynamics of a one-dimensional system of bosons with repulsive delta-function interaction. *Journal of Mathematical Physics*, 10(7):1115–1122, 1969.

[8] M. Gaudin. Thermodynamics of the Heisenberg-Ising ring for $\Delta >\sim 1$. *Phys. Rev. Lett.*, 26:1301–1304, May 1971.

[9] Toshiaki Iida and Miki Wadati. Exact analysis of -function attractive fermions and repulsive bosons in one-dimension. *Journal of the Physical Society of Japan*, 74(6):1724–1736, 2005.

[10] M T Batchelor, X W Guan, and J B McGuire. Ground state of 1d bosons with delta interaction: link to the BCS model. *Journal of Physics A: Mathematical and General*, 37(42):L497–L504, oct 2004.

[11] Y. Z. Jiang, Y. Y. Chen, and X. W. Guan. Understanding many-body physics in one dimension from the Lieb-Liniger model, 2015.

[12] M.D. Girardeau, Hieu Nguyen, and M. Olshanii. Effective interactions, fermi–bose duality, and ground states of ultracold atomic vapors in tight de Broglie waveguides. *Optics Communications*, 243(1):3–22, 2004. Ultra Cold Atoms and Degenerate Quantum Gases.

[13] X-W Guan and M T Batchelor. Polylogs, thermodynamics and scaling functions of one-dimensional quantum many-body systems. *Journal of Physics A: Mathematical and Theoretical*, 44(10):102001, Feb 2011.

[14] Olalla A. Castro-Alvaredo, Benjamin Doyon, and Takato Yoshimura. Emergent hydrodynamics in integrable quantum systems out of equilibrium. *Phys. Rev. X*, 6:041065, Dec 2016.

[15] Isabelle Bouchoule and Jérôme Dubail. Generalized hydrodynamics in the one-dimensional bose gas: theory and experiments. *Journal of Statistical Mechanics: Theory and Experiment*, 2022(1):014003, Jan 2022.

[16] Minoru Takahashi. Thermodynamical Bethe ansatz and condensed matter. *Lect. Notes in Phys.*, 498, 08 1997.

[17] Li Peng, Yicong Yu, and Xi-Wen Guan. Grüneisen parameters for the Lieb-Liniger and Yang-Gaudin models. *Phys. Rev. B*, 100:245435, Dec 2019.

[18] A Pavlis and X Zotos. Dressed excitations, thermodynamics and relaxation in the XXZ Heisenberg model. *Journal of Statistical Mechanics: Theory and Experiment*, 2020(1):013101, Jan 2020.

[19] X. Zotos. A TBA approach to thermal transport in the XXZ Heisenberg model. *Journal of Statistical Mechanics: Theory and Experiment*, 2017:103101, 2017.